Functional connectivity measures of scalp EEG and multimodal EEG-fMRI integration in epilepsy

João Pedro Isaías Abrantes
Under supervision of Patrícia Figueiredo and João Sanches
Dep. Physics, IST, Lisbon, Portugal

July 11, 2014

Abstract

Epileptic seizures are thought to be generated and to evolve due abnormal synchronization of the activity of neuronal populations, which reflects their functional connectivity. Therefore the study of these synchronizations may give valuable insights about the processes that rule these seizures. In particular, it would be useful to obtain measures of synchronization from the commonly recorded Electroencephalogram (EEG) signals. More specifically, these should be investigated as potential predictors of simultaneously recorded Blood-oxygen-level dependent (BOLD) signals measured using functional Magnetic Resonance Imaging (fMRI). In this work, different methods were developed to extract synchronization metrics out of EEG signals, including: linear correlation, nonlinear correlation (h^2) and phase-locking factor. These methods were then applied to EEG data recorded from a patient that has absence seizures with an unusual left hemisphere predominance in the associated spike-and-wave brain activity. The evolution of these metrics was analyzed over time, during ictal and inter-ictal periods, as well as in space, across the scalp topographies. The synchronization between close and distant pairs of electrodes was compared for different frequency bands. A greater local synchronization in the left posterior region of the brain was found to be present during the inter-ictal periods, while during the seizure the synchronization becomes stronger in the whole brain but most significantly in the left anterior region, consistently with the asymmetry of the seizure activity. Moreover, differences were found between synchronization on a low-frequency band ($\sim$ 3Hz) and a higher frequency band ($\sim$ 23Hz). The metrics were extracted from the EEG data recorded simultaneously with fMRI, and used as regressors of interest in a General Linear Model analysis done of the fMRI data. A Bayesian model comparison was performed, between the proposed synchronization metrics and other previously used EEG metrics, with the aim to identify which metric best models the BOLD dynamics during an epileptic seizure. The results did not show a significant difference between the tested metrics, possibly due to the fact that only one seizure was recorded using EEG-fMRI. In conclusion, EEG synchronization measures of brain functional connectivity were implemented and found to be sensitive metrics of ictal activity in a patient with left-lateralized absence seizures, providing insights into their temporal-spatial dynamics. Future work should further investigate the relationship between such EEG synchronization measures and the BOLD signal in a larger number of seizures and patients, also including other types of epileptic activity.

Keywords: Epilepsy; absence seizures; functional connectivity; synchronization; EEG; BOLD-fMRI;

1 Introduction

1.1 Epilepsy

Epilepsy is the second most common neurological disorder, staying only behind stroke, with a prevalence of 0.6-0.8% of the world's population. Two-thirds of the patients achieve sufficient seizure control from anti-convulsive medication, and another 8-10% could benefit from resective surgery, however for the remaining 25% of the patients, no sufficient treatment is yet available (Mormann et al., 2007). The most disabling aspect of the disease is the occurrence of sudden seizures that can cause convulsions, alter some brain functions and decrease the level of consciousness during the seizure time. The seizures can be partial, involving only part of the brain and producing symptoms in the corresponding body parts or in some related mental functions, or generalized, involving the whole brain, which is the case of the absence seizures (Tzallas et al., 2009).

The epileptic seizures are thought to be generated and to evolve through an underlying anomaly in the synchronization of the activity of different groups of neuronal populations (Mammone et al., 2012). Finding ways to extract and study this synchronization is therefore of crucial importance to understand the disease.

1.2 Electroencephalogram (EEG)

The main diagnostic and monitoring tool of the epilepsy condition is the Electroencephalogram (EEG). Using the EEG it is possible to record abnormal activity from patients, suffering from epilepsy, during iter-ictal periods (time between seizures) and ictal periods (during seizures). The EEG measures electric potential on the surface of the brain, which is the result of the sum of electrical activities from various populations of neurons within the brain, with a modest contribution from the glial cells. The neurons when activated produce time-varying electrical currents that produce electrical and magnetic fields at a certain distance from the neurons. In the case where the electrodes are placed on the scalp, the pyramidal cortex neurons will be the main contributors to the EEG signal, because they are aligned perpendicularly to the cortical surface and they form "open fields" (Niedermeyer and da Silva, 2005).

1.3 Functional Magnetic Resonance Imaging (fMRI)

Functional Magnetic Resonance Imaging (fMRI) applications to epilepsy have received considerable attention since epilepsy is, generally, a functional disorder that may not be accompanied by gross abnormalities in structural imaging. It's also important to use fMRI in order to identify key brain regions responsible for important functions such as language, memory, motion and others as part of the preoperative evaluation for epilepsy surgery (Detre, 2004). Most critically, the information retrieved by the fMRI exam can now be conjugated with the information retrieved by the EEG signal recorded simultaneously in order to characterize the evolution of a seizure or inter-ictal activity, in the so-called multimodal EEG-fMRI technique (Mulert and Lemieux, 2010).

The Blood Oxygen Level Dependent (BOLD) signal is most commonly measured in fMRI experiments, to obtained an indirect measure of brain activity (Jezzard and Toosy, 2005). When the neurons are in great activity they consume more oxygen which will decrease the local concentration of oxygen. To this local decrease of oxygen the brain responds with an increase of blood flow and with the expansion of the local blood vessels so that the level of oxygen in that area is not only enough to satisfy the demand but exceeds it. This increase in blood flow is local, it takes places around $2 \sim 3$ mm of the place where the neurons became more active (limiting the spatial resolution) and it will serve as an indirect mechanism of localization and measurement of brain activity. The fact that the hemoglobin, protein responsible for the transport of oxygen in the blood, has different magnetic properties whether it's binding oxygen (Hb) or not (deoxyhemoglobin dHb), will allow detecting differences in the oxygen concentration existing during brain activity and rest. The dHb has paramagnetic properties that make it more attractable to magnetic fields, perturbing them, and increasing the dephasing of the spins between water molecules and hence decreasing the decaying time T_2^* to

which the MRI signal is made sensitive (Logothetis and Wandell, 2004).

1.4 Synchronization metrics

The methods chosen to extract synchronization metrics out of the EEG recordings were the Phase Locking Value (PLV), linear correlation (R^2) and non-linear correlation (h^2). This choice was based on the sensitivity and consistency of the methods when evaluated in a previous report comparing different metrics in terms of their performance in the analysis of simulated data (Wendling et al., 2009).

1.5 Objectives

The main objective of this work is to develop and test methods for the extraction of synchronization metrics from the EEG data recorded from the scalp of epilepsy patients. These metrics will then be computed and analyzed on data collected from a patient with absence seizures that exhibit an unusual left hemisphere dominance.

Firstly, a total of 7 seizures recorded using a high-density 82-channels EEG system will be analyzed, in order to characterize the spatio-temporal dynamics of the associated synchronization. Secondly, one seizure recorded using a low-density 31-channels EEG system simultaneously with fMRI will be analyzed, in order to investigate the relationship between EEG synchronization and BOLD signal changes.

2 Methods

The data used in this work will first be described, followed by the presentation of the preprocessing steps that were taken. The computation of synchronization metrics is then presented, followed by the corresponding surrogate study. The specific analysis steps for the two major datasets used in this work are then also described.

2.1 Data Description

The EEG recordings used in this thesis are from a 11-year-old patient with absence seizures. These seizures usually occur for less than 20 seconds and start and end spontaneously. An absence seizure is characterized by the occurrence of spike-and-wave discharges (SWD) which generalize throughout the whole brain (Moeller et al., 2013). However in this patient there is an unusual asymmetry during the seizure where the left side of the brain is much more active than the right side.

2.1.1 High-density EEG data

Seven seizures were recorded using a high density EEG system with 82 channels and a sampling frequency of 500 Hz (SynAmps2, from Compumedics-Neuroscan) with AgCl electrodes included in an EasyCap with 74 positions from the system 10-10 plus electrodes on F11/12, FT11/12, TP11/12 and P11/12.

An illustrative example of a typical seizure from the patient studied is shown in figures 1 and 2. In figure, 1 the EEG signal timecourse is shown, where the typical spike-and-wave discharges are clearly recognized, with a particular incidence in the left hemisphere channels.

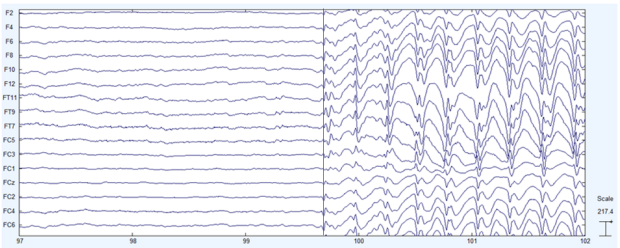

Figure 1: Time-courses of 16 representative channels of an epileptic seizure. The seizure onset is easily identified at 99.5 seconds (vertical red line).

In figure 2 the Wavelet time-frequency decomposition of the EEG signal is shown, exhibiting a higher power in frequencies around 3 Hz corresponding to the slow SWD typical of the absence seizures (Panayiotopoulos, 2001). We also see a periodical (3 Hz) increase in the intensity of higher frequencies ($\sim$ 16 Hz) that corresponds to the existence of fast spikes.

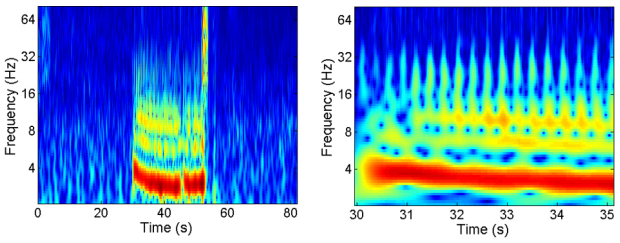

Figure 2: Power-spectrum of the timecourse in fig 1 (channel FC3), the onset of the seizure was now shifted to the 30th second. (Left) The full seizure is shown, between 30 and 50s, surrounded by two periods of baseline. (On the right) A zoom in was done to see the ictal period better.

2.1.2 Low-density EEG data with fMRI

One seizure was recorded simultaneously with fMRI and a low density EEG with 31 channels (BrainAmp MR-compatible system, Brain Products, Germany) with a sampling frequency of 250 Hz. The fMRI data were collected on a Siemens 3T system, using a gradient-echo echo planar imaging sequence, with $TR/TE = 2500/30$ ms, 240 volumes (total time; 10mins), and voxel size $3.75 \times 3.75 \times 5.00mm^3$ covering the whole brain.

2.2 EEG data pre-processing

The EEG signals were all originally referenced to the same EEG channel. This reference can cause an overestimation of the synchronization between channels because they're all related to this reference, and through it to each other. To overcome this problem, a Surface Laplacian was applied to the EEG (using the Matlab toolbox SSLTool), making the electrodes' signals independent of the reference. By eliminating this false synchronization the Surface Laplacian also effectively improves the spatial resolution of the EEG. It is fundamentally closely related to the local current density flowing radially through the skull into the scalp (Nunez, 1981).

Before the computation of the synchronization measures, the current density EEG data were filtered by a Finite Input Response (FIR) bandpass filter. When computing the PLV metric instead of the FIR filter a Morlet Wavelet was used. Both methods were used to obtain the following frequency bands:

- 2-4 Hz (low-frequency: centered around the spike-and-wave discharge frequency of $\sim$ 3 Hz and using a wavelet factor of 7);
- 14-18 Hz (high-frequency: centered around the frequency of the individual spikes of $\sim$ 16 Hz and using a wavelet factor of 7);
- 2-45 Hz (broadband: assumed to include all physiological information of interest; in this case the wavelet factor was 1.1 and the central frequency was 23.5 Hz);

2.3 Synchronization measures

2.3.1 Phase Locking Value (PLV)

Every signal $x(t)$ can be expressed in its analytical form $x_a(t) = A(t)e^{i\theta(t)}$, where $A(t)$ is the instantaneous amplitude and $\theta(t)$ is the instantaneous phase. This analytical form can be obtained by the Hilbert Transform or by a convolution with a wavelet (Quiroga et al., 2002). The PLV asserts the synchronization of two signals making the difference between their instantaneous phases along a temporal window. If the difference in the phases is constant along the window then the signals are synchronized, if the phases difference changes (with an uniform distribution) then the signals are not synchronized. Consider the two signals $x(t)$ and $y(t)$:

$$x(t) = A_x(t)e^{i\theta_x(t)} \tag{1}$$

$$y(t) = A_y(t)e^{i\theta_y(t)} \tag{2}$$

$$PLV = \frac{1}{N}|\sum_{n=1}^{N} e^{i(\theta_x(n)-\theta_y(n))}| \tag{3}$$

This method discards all the information contained in the instantaneous amplitude to assert the synchronization, so if the signals are coupled through the instantaneous amplitude the method will be insensitive to this coupling.

2.3.2 Correlation Coefficient (R^2)

The correlation coefficient may be the most used method to assess the synchronization/correlation between two signals, and it's also

one of the simplest.

$$r(x,y) = \frac{\sum_{i=1}^{n}(x_i - \bar{x})(y_i - \bar{y})}{\sqrt{\sum_{i=1}^{n}(x_i - \bar{x})^2}\sqrt{\sum_{i=1}^{n}(y_i - \bar{y})^2}} \quad (4)$$

where x and y are two different signals with n data points. When a signal rises at the same time as the other signal rises (decreases) we say that the two signals are correlated (anti-correlated). Both types of correlations correspond to synchronization between the signals, so we will often use the square of the correlation coefficient in order to have a value for the synchronization between 0 and 1.

2.3.3 Nonlinear correlation coefficient (h^2)

In this method we obtain a non-parametric measure of the nonlinear correlation between two signals. Consider two signals x and y, a plot of y versus x will be studied. x will be divided into bins and for each bin we will have a point (p_i, q_i) where p_i is the x midpoint of the bin and q_i is the average of the y values contained by the bin. By connecting all the resulting points (p_i, q_i) with linear segments we obtain the curve $f(x_i)$. The h^2 coefficient is then computed as follows (Pereda et al., 2005):

$$h^2_{y|x} = \frac{\sum_{k=1}^{N} y(k)^2 - \sum_{k=1}^{N}(y(k) - f(k))^2}{\sum_{k=1}^{N} y(k)^2} \quad (5)$$

Besides giving us information about the correlation of two signals, the h^2 metric can also give us information about the possible causality between signals. For example, the computation of $h^2(\sin^2(t), \sin(t))$, being t a time vector, is equal to zero because there isn't any non-linear function that can transform the signal $\sin^2(t)$ into $\sin(t)$. However the inverse isn't true, there is a non-linear function (the square) that can transform the signal $\sin(t)$ into $\sin^2(t)$, so $h^2(\sin(t), \sin^2(t))$ is equal to one. A signal $\sin(t)$ is capable of causing a $\sin^2(t)$ response, but the opposite isn't true. If this asymmetry of the h^2 is exploited this method may also be able to extract the effective connectivity of the brain.

2.4 Surrogate Study

To assert the significance of the measures yielded by the different synchronization methods, a surrogate study was conducted as follows. In this context, a surrogate is a transformation of a signal that shares some properties of its original, such as the mean, the variance, the spectral composition and the power. However the surrogate isn't synchronized with the original signal. To create a surrogate the method described in (Theiler et al., 1992) was used. We took the original signal from one of the EEG channels, a typical signal similar to the signals analyzed throughout this paper. We took the Fast Fourier Transform (FFT) of that signal and for each component we randomized its phase. In order for the surrogate signal to be real we need to make sure that the phases, ϕ, are symmetrical, in the frequency f, i.e. $\phi(f) = -\phi(-f)$. We should also be careful and guarantee that there isn't a big discontinuity from the last point of the original signal to the first, because when doing a FFT it is assumed that the signal is periodic with period N. Therefore, if there is a discontinuity in the signal, x, between $x(N-1)$ and $x(0)$, then spurious high frequencies will be introduced. In this work the average (μ) difference between neighbor points and the corresponding standard deviation (σ) was computed, the last point was then chosen so that the difference between it and the first point would be less than $\mu + \sigma$. Doing the Inverse Fast Fourier Transform (IFFT) the surrogate signal is obtained where its Fourier spectrum is equal to the original in terms of amplitude but its phase is scrambled across time destroying any synchronization between the two signals.

We can now apply each of the synchronization methods to the original signal and its surrogates, and then test the significance of the synchronization in contrast with the null hypothesis (i.e. the two signals are not synchronized). The synchronization measures can then be expressed in terms of its significance, as z-score (number of standard deviations away from the mean) in relation to the surrogates.

The surrogates methodology is employed here on one representative EEG signal, in order to investigate the effect of the window size on the significance of the results. The surface Laplacian

was first applied, and the resulting signal was band filtered for the different frequencies bands described in section 2.2. The process of surrogate generation was repeated 10 times and the respective average and standard deviation of all surrogate signals were then taken, as is shown in figures 3 and 4.

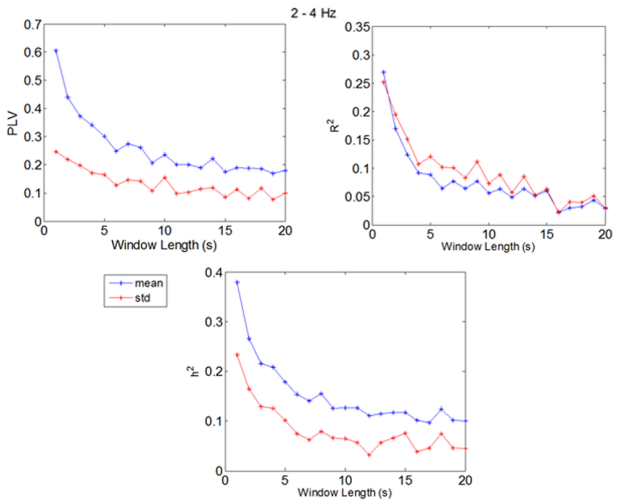

Figure 3: Synchronization measures applied to the surrogates of a representative EEG signal, filtered to 2-4 Hz, for window sizes varying between 1 and 20s.

As expected, increasing the window size decreases the mean but also the standard deviation, leading to more significant measures. The PLV is the method that has a larger mean for all the different time window sizes. This result shows that the PLV is the method with the highest bias (in agreement with Wendling et al. (2009)), where the linear correlation is the one with the lowest bias.

Comparing the figures 3 and 4 we see that the mean of the null hypothesis is much lower when the frequency band is wider. This may be due to the fact that, when the frequency band is wider we now have more Fourier components to scramble their phases, making it less probable to have two synchronized signals by chance.

The results of the synchronization measures from now on will be expressed as a z-score in respect to the surrogate data.

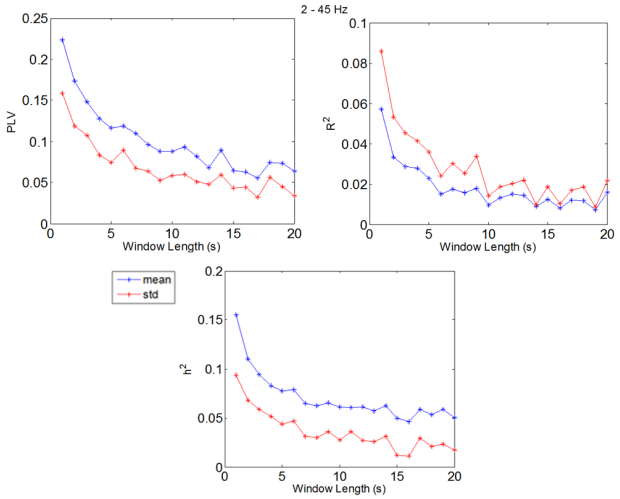

Figure 4: Synchronization measures applied to the surrogates of a representative EEG signal, filtered to 2-45 Hz, for window sizes varying between 1 and 20s.

2.5 EEG-fMRI analysis (low-density EEG data)

The pre-processing of the fMRI images was done using the FSL software and consisted in the following procedures: brain-extraction (by the Brain Extraction Tool (BET)), motion correction (MCFLIRT), spatial smoothing (using a Gaussian kernel with a Full Width at Half Maximum (FWHM) of 5mm) and temporal filtering (high-pass filter of 100s).

Using the metrics extracted from the EEG, a General Linear Model (GLM) was performed in the fMRI data (by the Matlab toolbox SPM). To compare the metrics and see which one best models the BOLD dynamics a Bayesian Model Comparison was performed (also using SPM).

3 Results

3.1 High Density EEG

The results obtained by applying the synchronization measures implemented in this work to the EEG data of a patient with left-lateralized absence seizures are presented here. Firstly, the high-density EEG data of a group of 7 seizures is presented, and then the low-density EEG data of one seizure recorded with fMRI is analyzed.

An EEG data segment of 60s was extracted

around each of the seven seizures, so that the seizure onset is at 30s, always preceded by an inter-ictal period of 30s and followed by a seizure of variable duration (between 2s and 22s). The synchronization of the EEG signal at each electrode with its N_{close} closest neighbors (close synchronization) and with its $N_{far} = 81 - N_{close}$ furthest neighbors (far synchronization) was computed and averaged for each seizure and then averaged across seizures, each seizure has a different duration the average makes sense only for the baseline preceding the seizure and the seizure onset time. Different values of N_{close} (and N_{far}) values were tested and the value $N_{close} = 67$ ($N_{far} = 14$) was selected to distinguish the close synchronization from the far because it maximized the difference between the metrics in the inter-ictal and the ictal period. The mean synchronization measures for the 7 seizures are shown in figure 5. It's observable that the difference between the close and far synchronization gets smaller during the seizure which may also be a good metric to describe the seizure. Right before the seizure onset there's a small rise on this difference (Close - Far, graph not shown here) and a significant dip when the seizure starts. This may mean that the close synchronization is the first to rise, followed by the far synchronization, nearly matching.

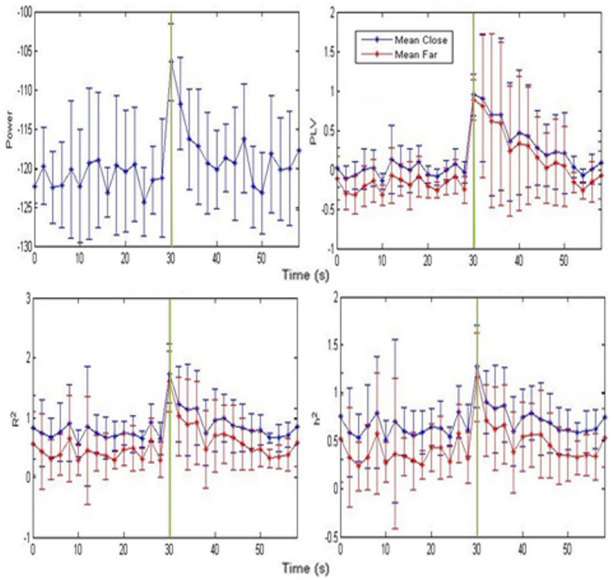

Figure 5: Mean synchronization measures (z-scores) computed for each time point of the 60s segment around the 7 seizures (error bars represent standard deviation). The data was band-pass filtered (2-4 Hz). The beginning of the seizures are represented by the green vertical lines.

The p-values of the t-test between the synchronization measures in the baseline and seizure periods, across the 7 seizures, are shown in figure 6.

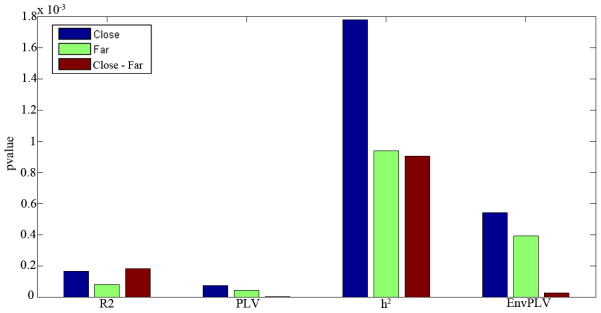

Figure 6: Comparison between seizure and baseline: the p-value of the different synchronization metrics averaged across close channel pairs and far channel pairs, as well as as their difference.

All the p-values are less than 0.05 meaning that the probability of the two sets of datapoints (from the seizure and from the baseline) being generated by the same distribution is very unlikely. The methods have similar performances but the one that yields the lowest p-value is the PLV and it will be the one mostly used in this work.

To investigate the behavior of the synchronization in different frequency bands a time-frequency analysis was performed (figure 7).

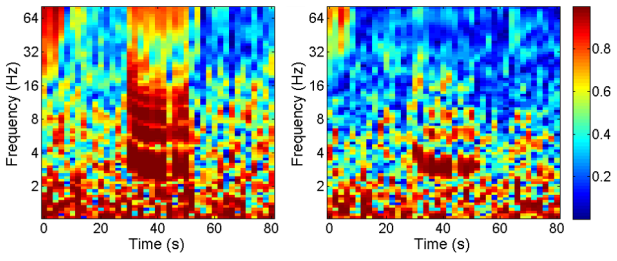

Figure 7: Time-frequency analysis of the synchronization (PLV) of two (Left) nearby EEG channels (F3 and F5) and (Right) distant EEG channels (F5 and F4) from an epileptic seizure starting at 30s and ending at 52s.

The synchronization of the close channels is similar to the time-frequency analysis done to the power of the signal showed in figure 2. The synchronization of the distant pair doesn't intensify

as much for the high frequencies as the close pair does. This result complies with the observations seen in Dominguez et al. (2005) where it was found that the high frequency synchronization occurs more locally than the low frequency synchronization. The synchronization of each pair of channels is plotted as function of their distance in figure 8.

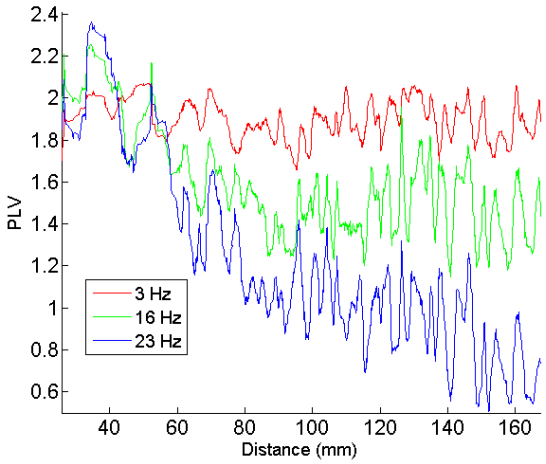

Figure 8: PLV synchronization of each pair of channels in function of their distance. The graph was smoothed with a Gaussian filter.

Figure 8 shows that the low frequency synchronization is constant in function of the distance while the synchronization in the high frequencies decreases with the distance. For distances greater than 60mm the synchronization in the high frequencies is less than 1.6 (z-score computed in respect to the surrogate data) meaning that the synchronization is not significant. We will also use 60mm as a threshold to distinguish the close pairs from the far.

In order to study the temporal and spatial distribution of the synchronization, topographic plots were made for all the different seizures, the image 9 shows an example of one of those plots. Each circle in the topographic plot represents an EEG channel, and the value inside the circle represents it's average synchronization with its close neighbors.

In figure 9 it's observable a higher synchronization on the left posterior region of the brain during inter-ictal periods. On the seizure onset the synchronization becomes higher and more homogeneous across the brain having however slightly

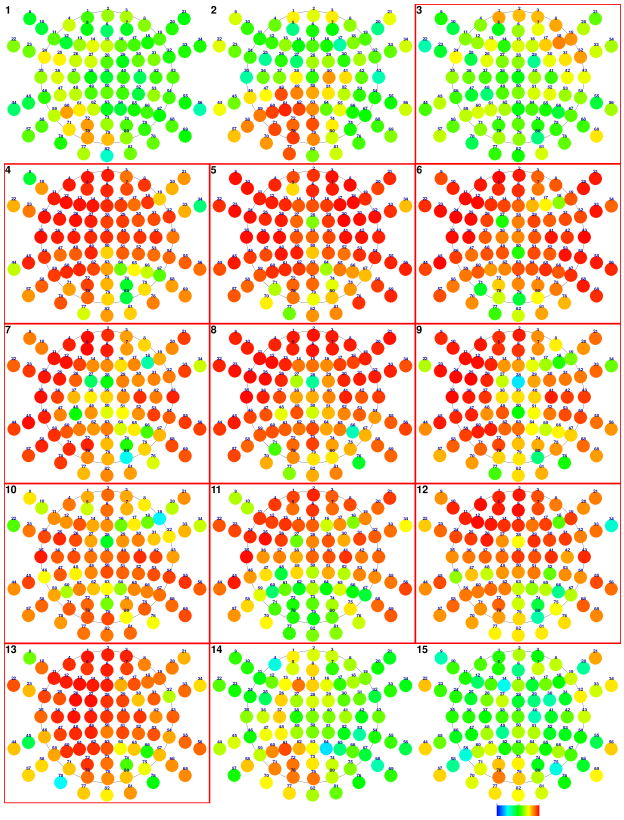

Figure 9: The average synchronization (obtained using PLV) of each channel with its close neighbors (with a distance lower than 60mm), averaged for different time windows with the duration of 2 seconds each. The temporal evolution goes from left to right, top to bottom. The topographies within a red square occur during the seizure period. The signal was low-pass filtered by means of a convolution with a Morlet Wavelet with central frequency set at 3Hz and a wavelet factor $R = 7$.

bigger values in the left anterior part of the brain which is in tune with the asymmetry found by the patient's doctors.

To resume the data of all the topographies created, using different frequency bands and different neighbors ranges from all seizures, the histogram in figure 10 was created.

The synchronization during the inter-ictal period is higher in the left posterior region and at the beginning of the ictal period, the synchronization increases more significantly in the anterior region than in the posterior region. At higher frequencies, the synchronization in the left posterior actually decreases at the seizure onset.

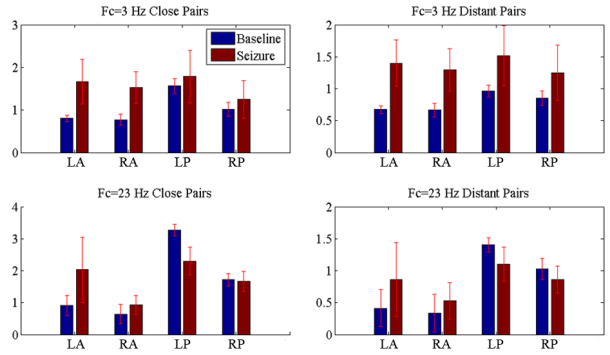

Figure 10: The synchronization (PLV) for different brain regions and for different frequency bands assessed for the close and distant pairs. Fc stands for central frequency used in the Morlet wavelet, with a wavelet factor of 7. The average across inter-ictal data-points are represented by the blue bars while the red bars illustrate the average from the first point across the ictal periods. LA (Left Anterior), RA (Right Anterior), LP (Left Posterior), RP (Right Posterior).

3.2 Low Density EEG and EEG-fMRI

For the low density EEG signal bivariate metrics were obtained: PLV, R^2 and the PLV of the envelope of the signals (envPLV). Additionally, univariate metrics such as the power, instantaneous frequency and a boxcar function describing the seizure were also extracted. Each metric was then convolved with the canonical haemodynamic response function (metrics in figure 11), and used as regressor of interest in separate GLM analyses of the BOLD-fMRI data using the SPM toolbox from MATLAB. Additionally, six confounding regressors estimated from MCFLIRT algorithm were included to account for BOLD signal changes related to head movements.

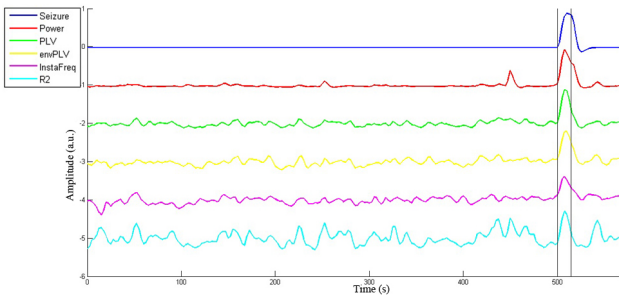

Figure 11: The timecourse of each of the regressors used in the GLM.

To compare the metrics a Bayesian Model Comparison was done using the SPM toolbox. A bayesian model estimation was done for each metric resulting in a log evidence map which gives the probability of the data being generated by the model, described by the regressor of the specific metric and six regressors to account for motion artifacts. The posterior probability, the probability of a model given the data, was then computed assuming equal priors (the priori probability of each model is assumed to be the same).

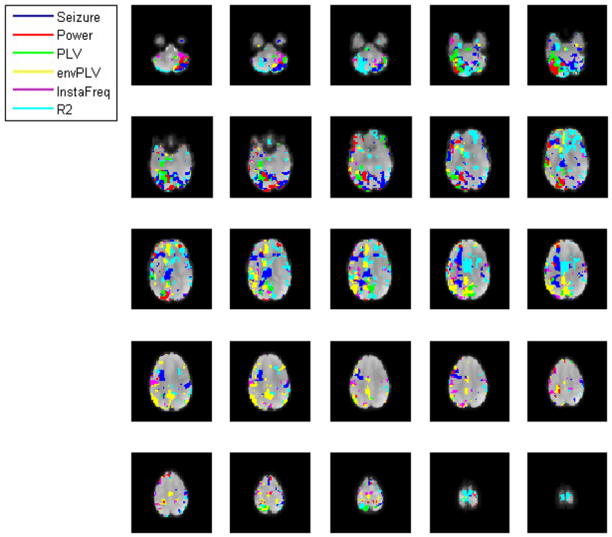

Figure 12: Representative slices where each voxel was colored with the color of the metric that had the greatest posterior probability. A mask was applied so that only the voxels where some metric obtained a p-value less than 0.05, in the GLM analysis, were painted.

The BOLD signal changes during an absence seizure have been studied in Moeller et al. (2010). A thalamic activation was very often found (in 96% of the seizures studied), deactivations in the default mode areas (88%) and in the caudate nuclei (59%). There have been also documented cortical activations in patient-specific areas (59%). The results obtained (figure 12) from our data comply with the results found by Moeller; the seizure (metric) is strongly positive correlated with the thalamus, the R^2 is negatively correlated with the caudate nuclei and the power is correlated with some positive cortical areas.

The models give similar results however in some areas some models are significantly more probable then others. The posterior probabil-

ity of the best model in the voxels within the thalamus and caudate nuclei is bigger than 60% showing that these models are significantly better correlated with these voxels than the other models.

4 Discussion

In this work, several synchronization metrics were tested in both high and low-density EEG signals recorded from a drugs-refractory patient with left-lateralized absence seizures. Each of the synchronization metric demonstrated to have discriminative power in distinguishing ictal from baseline periods, also capturing the asymmetric spatial distribution of epilepsy-related electric potentials which is in agreement with the information gathered from the patient's doctor. According to the surrogate study, the PLV was the most biased synchronization metric and yet provided with the highest sensitivity for detecting changes occurring during the seizure.

High frequency synchronization was found to occur locally while low frequency synchronization occurs more generally throughout the brain.

The higher synchronization in left posterior region of the brain during the inter-ictal periods and the decrease of this synchronization in the beginning of the seizures, for high frequency bands, is a very curious phenomenon and it would be very interesting to see if a pattern could be found in seizures from other patients with absence seizures.

For the low-density EEG datasets, simultaneous BOLD-fMRI data was also acquired. By means of a GLM analysis where each metric was defined as a regressor of interest, it was possible to correlate synchronization measures with BOLD signal changes within the expected brain regions. However a very simple metric such as the seizure metric (one during the ictal period and zero elsewhere) was found to be more strongly correlated with the thalamus than the other more complex metrics.

Finding the origin of an absence seizure is a problem that many thought to be impossible. However new researches (Westmijse et al. (2009), Meeren et al. (2002)) suggest that the origin of an absence seizure does exist but its propagation and generalization is so fast that it's hard to capture it. In this work, only measures of functional connectivity were computed but the causality of these connections are intended to be exploited in the future. We would need to use much shorter time windows to capture the fast propagation, however our surrogate study shows that we need to use a broader and higher frequency band in order to obtain significant synchronization measures for short time windows. Taking into account that the low-density EEG contained a limited number of data-points in which a seizure was captured, the asymmetry in both the EEG h^2 metric and the fMRI effective connectivity estimation by DCM did not allow significant conclusions about the causality of the system.

In conclusion, the selected EEG synchronization measures of brain functional connectivity (R^2, h^2 and PLV) were successfully implemented and found to be sensitive to ictal activity in a patient with left-lateralized absence seizures, providing new insights into their temporal-spatial dynamics. Both bivariate and univariate metrics were found to be spatially correlated with BOLD signal changes for regions that are anatomically known to play an important role in the generation and evolution of absence seizures. Further work including more data is necessary in order to investigate whether EEG synchronization measures may help explain BOLD changes associated with epileptic activity.

References

Detre, J. A. fMRI: applications in epilepsy. *Epilepsia*, 45(s4):26–31, 2004.

Dominguez, L. G., Wennberg, R. A., Gaetz, W., Cheyne, D., Snead, O. C., and Velazquez, J. L. P. Enhanced synchrony in epileptiform activity? Local versus distant phase synchronization in generalized seizures. *The Journal of neuroscience*, 25(35):8077–8084, 2005.

FSL. Fsl. http://fsl.fmrib.ox.ac.uk/. Accessed: 2014-02-25.

Jezzard, P. and Toosy, A. *Functional MRI*. Springer, 2005.

Logothetis, N. K. and Wandell, B. A. Interpreting the BOLD signal. *Annu. Rev. Physiol.*, 66: 735–769, 2004.

Mammone, N., Labate, D., Lay-Ekuakille, A., and Morabito, F. C. Analysis of absence seizure generation using EEG spatial-temporal regularity measures. *International journal of neural systems*, 22(06), 2012.

Meeren, H. K., Pijn, J. P. M., Van Luijtelaar, E. L., Coenen, A. M., and da Silva, F. H. L. Cortical focus drives widespread corticothalamic networks during spontaneous absence seizures in rats. *The Journal of neuroscience*, 22(4):1480–1495, 2002.

Moeller, F., LeVan, P., Muhle, H., Stephani, U., Dubeau, F., Siniatchkin, M., and Gotman, J. Absence seizures: individual patterns revealed by EEG-fMRI. *Epilepsia*, 51(10):2000, 2010.

Moeller, F., Stephani, U., and Siniatchkin, M. Simultaneous EEG and fMRI recordings (EEG-fMRI) in children with epilepsy. *Epilepsia*, 54 (6):971–982, 2013.

Mormann, F., Andrzejak, R. G., Elger, C. E., and Lehnertz, K. Seizure prediction: the long and winding road. *Brain*, 130(2):314–333, 2007.

Mulert, C. and Lemieux, L. EEG-fMRI. *Physiological Basis, Technique and Applications*, 2010.

Niedermeyer, E. and da Silva, F. L. *Electroencephalography: basic principles, clinical applications, and related fields*. Lippincott Williams & Wilkins, 2005.

Nunez, P. L. Electric fields of the brain: The neurophysics of EEG, 1981.

Panayiotopoulos, C. Treatment of typical absence seizures and related epileptic syndromes. *Paediatric drugs*, 3(5):379–403, 2001.

Pereda, E., Quiroga, R. Q., and Bhattacharya, J. Nonlinear multivariate analysis of neurophysiological signals. *Progress in neurobiology*, 77 (1):1–37, 2005.

Quiroga, R. Q., Kraskov, A., Kreuz, T., and Grassberger, P. Performance of different synchronization measures in real data: a case study on electroencephalographic signals. *Physical Review E*, 65(4):041903, 2002.

SSLTool. Ssltool. http://ssltool.sourceforge.net/. Accessed: 2014-02-25.

Theiler, J., Eubank, S., Longtin, A., Galdrikian, B., and Doyne Farmer, J. Testing for nonlinearity in time series: the method of surrogate data. *Physica D: Nonlinear Phenomena*, 58(1): 77–94, 1992.

Tzallas, A. T., Tsipouras, M. G., and Fotiadis, D. I. Epileptic seizure detection in EEGs using time–frequency analysis. *Information Technology in Biomedicine, IEEE Transactions on*, 13 (5):703–710, 2009.

Wendling, F., Ansari-Asl, K., Bartolomei, F., and Senhadji, L. From EEG signals to brain connectivity: a model-based evaluation of interdependence measures. *Journal of neuroscience methods*, 183(1):9–18, 2009.

Westmijse, I., Ossenblok, P., Gunning, B., and Van Luijtelaar, G. Onset and propagation of spike and slow wave discharges in human absence epilepsy: a meg study. *Epilepsia*, 50(12): 2538–2548, 2009.